

Analysis of 5G RAN Configuration to Support Advanced V2X Services

M. Carmen Lucas-Estaf¹, Baldomero Coll-Perales¹, Takayuki Shimizu², Javier Gozalvez¹, Chang-Heng Wang², Bin Cheng², Miguel Sepulcre¹, Sergei Avedisov², Takamasa Higuchi², Onur Altintas²

¹Uwcore laboratory, Universidad Miguel Hernandez de Elche, Elche (Alicante), Spain.

²InfoTech Labs, Toyota Motor North America R&D, Mountain View, CA, U.S.A.

¹{m.lucas, bcoll, j.gozalvez, msepulcre}@umh.es

²{takayuki.shimizu, chang-heng.wang, bin.cheng, sergei.avedisov, takamasa.higuchi, onur.altintas}@toyota.com

Abstract—5G offers high flexibility at the radio, transport and core networks to support various services of critical verticals such as connected and automated driving. At the Radio Access Network (RAN), 5G defines a New Radio (NR). 5G NR utilizes different subcarrier spacing, slot durations, modulations and channel coding schemes. This flexibility offers the possibility to support automotive services with different and demanding requirements, such as Advanced Driver-Assistance System (ADAS), cooperative driving, and remote driving. Previous studies showed that 5G NR can be configured to achieve latencies below 2 ms. However, existing studies are generally restricted to scenarios with a limited number of users and unlimited bandwidth. Therefore, it is important to analyze whether 5G NR can effectively support these services as the network scales under limited spectrum allocations. This study advances the current state of the art to demonstrate that the capability of 5G NR RAN to support advanced V2X services depends on the RAN configuration (subcarrier spacing, slot duration and error protection) and network load.

Keywords—5G, NR, New Radio, RAN, 5G V2X, V2X, Vehicle to Everything, V2N, V2N2V, connected automated vehicles, CAV.

I. INTRODUCTION

5G systems have been designed to be highly flexible and support advanced services with stringent bandwidth, reliability and latency requirements. To this aim, 5G defines a New Radio (NR) interface that includes new subcarrier spacing (SCS), slot durations, modulations and channel coding schemes. The capabilities of 5G have raised expectations on its potential to support highly demanding services such as those related to connected and automated driving (e.g., Advanced Driver-Assistance System -ADAS-, cooperative driving, or remote driving).

Several studies have already analyzed the performance of the 5G NR Uu interface¹ for uplink (UL) and downlink (DL). For example, the 3GPP's Technical Specification Group Radio Access Network (RAN) evaluated in [1] the latency that can be achieved at the radio network considering the transmission of small IP packets in unloaded conditions. The study demonstrated that 5G NR can achieve UL and DL latency values below 2 ms using different RAN configurations (FDD or TDD frame structure, different numerologies and slot formats). The study in [1] also shows that lower latency values (<1 ms) can be achieved using higher numerologies, even when using a 14-symbol slot. Over-the-air latency values below 2 ms have also been demonstrated in proof-of-concept trials presented in [2] for Vehicle-to-Network-to-Vehicle

(V2N2V) connections between trucks operating a platoon. The study in [3] also showed that latency values below 2 ms can be achieved with different numerologies. [3] also showed that the latency can increase with the numerology due to the increase of signaling exchange, and that this depends on the particular traffic pattern. All these previous results show that 5G NR can meet stringent latency requirements of highly-demanding services such as advanced V2X (also referred to as enhanced V2X or eV2X). However, these results have been achieved under limited and controlled scenarios, and it is still necessary to evaluate and understand the 5G NR performance under realistic operating conditions with different network loads. To this aim, the authors analyzed in [4] the scalability and latency of the 5G NR RAN as a function of the vehicle density and packet size. The results in [4] demonstrated that the capability of the 5G NR RAN to support advanced V2X services can be compromised as the network scales. The study in [4] considered a particular configuration of 5G NR, and it is then necessary to supplement this study by investigating 5G NR configurations that can better support advanced V2X services at scale. This study advances the state of the art with the evaluation of the impact of the 5G NR configuration on the scalability of 5G networks for advanced V2X services. In particular, this paper analyzes the latency, reliability and spectrum efficiency that can be achieved at the RAN (excluding the transport network) with different 5G NR numerologies, slot durations, cyclic prefixes, and modulation and coding schemes. Furthermore we consider V2X services with different requirements that relate to the level of automation of CAVs (Connected Automated Vehicles). The impact of the 5G NR configuration is analyzed as the network scales with the density of vehicles and the traffic load generated per vehicle.

II. LATENCY AT THE 5G NR RAN

5G NR defines multiple numerologies and two different cyclic prefixes that result in different symbol durations. The numerologies consider different subcarrier spacings (SCS) in the frequency domain and slot durations in the time domain as defined in [5]. The slot duration ranges from 1 ms for numerology 0 with 15 kHz SCS to 0.0625 ms for numerology 4 with 240 kHz SCS. The channel bandwidth is divided into Resource Blocks (RBs) of 12 subcarriers each. To estimate the latency at the 5G NR RAN, we use the model presented in [4]. This model computes the RAN latency as the sum of the UL latency in the transmission from the User Equipment (UE) to the gNB (or base station), and the DL latency in the

¹ The Uu interface is the radio interface between the User Equipment (UE) and the Radio Access Network (RAN).

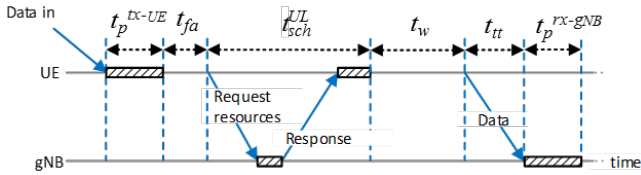


Fig. 1. Latency in the UL transmission of a packet. Striped rectangles represent the processing of packets in the UE or gNB [4].

transmission from the gNB to the UE. The UL and DL latencies are estimated by considering all delay components represented in Fig. 1 for the UL transmission of a packet. These are explained below for UL transmissions but a similar process is followed to compute the DL latency.

Processing delay at transmitter (t_p^{tx-UE} for UL) and receiver (t_p^{rx-gNB} for UL). For the transmitter, this delay represents the time necessary to generate a packet, while at the receiver it accounts for the time necessary to decode a received packet. The processing delay at the transmitter (UE for UL or gNB for DL) is equal to $T_{proc,2}/2$ following [1], where $T_{proc,2}$ is the Physical Uplink Shared Channel (PUSCH) preparation procedure time. The processing delay at the receiver (gNB for UL or UE for DL) is equal to $T_{proc,1}/2$ following [1], where $T_{proc,1}$ is the Physical Downlink Shared Channel (PDSCH) processing procedure time.

Frame alignment time (t_{fa}). t_p^{tx-UE} in UL might be completed at any time within a slot. To estimate the RAN latency, it is also necessary to account for the frame alignment time t_{fa} until the start of the next slot. t_{fa} is limited by the duration of the slot.

Delay introduced by the scheduling (t_{sch}^{UL} in UL and t_{sch}^{DL} in DL). This study considers the use of Semi-Persistent Scheduling (SPS) scheme for DL transmissions and Configured Grant (CG) scheduling for UL transmissions². SPS and CG pre-assign resources periodically for a UE when the UE attaches to the gNB. In this study, we consider that the periodicity between allocated resources is set equal to the time interval between two successive data packets. In this case, t_{sch}^{UL} and t_{sch}^{DL} are null since the UE does not have to request resources to transmit each packet.

Waiting time for the allocated RBs (t_w). The RAN latency must also account for the waiting time t_w until the slot where RBs are assigned to the UE. t_w depends on the number of RBs needed to transmit a packet that is a function of the packet size, the Modulation and Coding Scheme (MCS), and the number of MIMO transmission layers. This study adapts the MCSs based on the Channel Quality Indicator (CQI) that is estimated as a function of the distance between the vehicle and the serving gNB. We consider the MCS and CQI tables (1, 2 or 3) specified in [6]. The MCS is adapted to achieve a Block Error Rate (BLER) target equal to 10% when using tables 1 or 2 from [6]. With table 3, the MCS is adapted to guarantee a BLER of 10^{-5} . t_w also depends on the number of RBs available at each slot that is a function of the bandwidth and the numerology following [7]. To estimate this number, we must eliminate those RBs used by control channels and PHY signals (Demodulation Reference Signals, Channel Status Information, and Sounding Reference Signals)

following the configuration specified in [8]. The rest of RBs can be used for data transmissions. This study emulates the resource allocation process to identify the number of RBs available at each slot as a function of the vehicular density. t_w is then estimated numerically considering that the scheduler allocates RBs in the first slot where there are sufficient available RBs to transmit the packet.

Transmission time (t_{tt}). Finally, the latency must also account for the transmission time, which is equal to the duration of the slots (previously estimated) necessary to transmit the data packet. The duration of a slot depends on the NR numerology.

III. EVALUATION SCENARIO

We consider for this study the cooperative lane change service that is part of the advanced driving group identified by 3GPP under [9]. This document specifies the performance requirements for connected and automated driving eV2X services. Cooperative lane change requires vehicles to exchange driving intentions or maneuver coordination messages with nearby vehicles so that they can coordinate their trajectories and maneuvers. Cooperative lane change has been traditionally supported using Vehicle to Vehicle (V2V) communications (e.g. [10]). However, it is interesting to investigate the feasibility of supporting it using 5G networks (through V2N2V communications) considering the technical capabilities and flexibility introduced by 5G networks, and particularly 5G NR at the RAN.

The format, length, and periodicity of the cooperative lane change messages have not yet been decided and are under study in 3GPP TS 22.186 [9], ETSI TR 103 578 (v0.0.5), and SAE J3186. Discussions currently consider a possible message size of 300 to 600 bytes [11]. [9] defines requirements for the cooperative lane change service depending on the level of automation that reflects functional aspects. [9] makes a distinction between lower levels and higher levels of automation based on whether the human operator or the automated system is primarily responsible for monitoring the driving environment. For a high level of automation (HLoA), 3GPP requires messages to be exchanged between vehicles with less than 10 ms latency and with 99.99% reliability. The reliability is defined as the percentage of packets successfully delivered to a given node within the time constraint required by the targeted service. Requirements are relaxed when vehicles support a low level of automation (LLoA). In particular, the end-to-end latency requirement is relaxed to 25 ms and the reliability requirement is reduced to 90%.

We consider a highway scenario and a 5G NR cell radius of 866 m following [12]. The cell is assigned 40 MHz bandwidth in UL and DL in the Frequency Range 1 (FR1)³. The highway consists of 6 lanes per direction, and we evaluate vehicle densities equal to 20, 60, and 80 vehicles/km/lane corresponding to different traffic flow conditions (free-flow, stop and go, and congestion). Vehicles periodically exchange messages of 300 bytes with a transmission period T_p equal to 20, 50, or 100 ms. The messages include information about the vehicles' planned or desired trajectories so that they can coordinate their maneuvers. Messages are exchanged using 5G V2N2V communications but all the application's

² Dynamic scheduling introduces a signaling latency to request resources for each transmission that may compromise certain critical V2X services.

³ The configured bandwidth is only used for V2X traffic.

processing is done at the vehicles. Vehicles then send the messages to the gNB, and the gNB forwards the data to the neighboring vehicles using broadcast communications. Broadcast communications are not supported in 3GPP Release 15 or Release 16 but are being studied together with multicast communications under Release 17 [13] since both communication modes are highly relevant (and necessary) to efficiently support V2X services (among others).

We evaluate the performance of 5G NR to support advanced V2X services using different FR1 numerologies (μ). In particular, we evaluate numerologies 0, 1, and 2 defined in [5] and presented in Table I. Numerologies 0 and 1 always use normal cyclic prefix (NCP). On the other hand, numerology 2 can use either NCP or extended cyclic prefix (ECP). This study considers the use of numerology 2 with ECP to better combat inter-symbol interference (ISI) in the scenario given the large cell radius⁴. The UE processing capability is equal to 2, and $T_{proc,1}$ and $T_{proc,2}$ take values equal to 0.161 and 0.193 ms, respectively [6]. We consider full-slot transmissions in UL and DL and two MIMO transmission layers. This study evaluates the performance achieved with the MCS and CQI table 2 defined in [6] that has a target BLER equal to 10%, and with the MCS and CQI table 3 defined in [6] that has a target BLER equal to 10^{-5} . The use of MCS and CQI table 2 can be considered as a Low Error Protection (LEP) configuration, and it can support in principle the requirements of cooperative lane change with low level of automation. On the other hand, the use of MCS and CQI table 3 can be considered as a High Error Protection (HEP) configuration, and it can support in principle the requirements of cooperative lane change with high and low levels of automation. In both configurations, vehicles adapt the MCS as a function of the CQI to achieve the target BLER. The CQI is estimated as a function of the distance between the vehicle and the serving gNB.

TABLE I
EVALUATED NUMEROLOGIES

Numerology (μ)	Subcarrier Spacing (SCS)	Cyclic prefix	Number of OFDM symbols per slot	Slot time duration [ms]
0	15	Normal	14	1
1	30	Normal	14	0.5
2	60	Extended	12	0.25

IV. PERFORMANCE EVALUATION

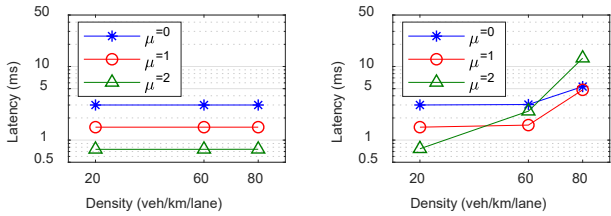
This section analyzes the performance that can be achieved using different configurations of the 5G NR RAN, and identifies which configurations can satisfy the service requirements for the two different levels of automation. Fig. 2 shows the average latency experienced for different numerologies and vehicle densities when $T_p=50$ ms. We should note that the figure plots the latency for the packets that are transmitted and are not dropped. In this study, a packet is dropped if it is not transmitted (e.g., because there are no RBs available for the transmission) by the time a new packet is generated at the transmitter. This is because the cooperative lane change service requires vehicles to use the latest and most updated information to coordinate their maneuvers. If a vehicle wants to transmit a packet with its position and trajectory at a given moment in time, and the previous packet (that included the previous position and trajectory) has not yet been transmitted, the vehicle must drop the previous packet,

otherwise it would send outdated information to the vehicle it wants to coordinate its maneuver with (packets dropped for the different RAN configurations will be investigated later in this section). Fig. 2.a depicts the latency for the low error protection (or LEP) configuration, and Fig. 2.b shows the latency for the high error protection (or HEP) configuration. Fig. 2 shows that similar latency values are obtained for LEP and HEP when the density of vehicles is low (20 veh/km/lane). The latency experienced with the LEP configuration (BLER target=10%) is not significantly affected by the vehicular density. However, it significantly increases with the HEP configuration that has a BLER target of 10^{-5} . The latency increases with HEP for all the numerologies analyzed. This is because increasing the error protection to guarantee a lower BLER requires using more robust MCSs that need a higher number of RBs to transmit each packet. This is visible in Table II that shows the average number of RBs needed to transmit a packet of 300 bytes when using the LEP and HEP configurations. The use of a higher number of RBs to transmit each packet with HEP increases the percentage of utilized RBs (and hence the channel load). This is observed in Fig. 3 that represents the percentage of RBs utilized as a function of the vehicular density for the LEP and HEP configurations. Fig. 3 shows that at densities of 20 and 60 veh/km/lane the HEP configuration uses 168% and 155% more RBs than the LEP configuration. Fig. 3 also shows that the percentage of utilized RBs increases with the density as expected. However, such increase has almost no impact on the latency when using the LEP configuration (Fig. 2.a), while it significantly increases the latency when using the HEP configuration (Fig. 2.b). This is because the usage of RBs is maintained below 50% with LEP for all vehicular densities analyzed. On the other hand, the percentage of RBs utilized when using the HEP configuration is higher than 77% for all numerologies when the vehicular density is equal to 60 veh/km/lane. This percentage increases to almost 100% for all numerologies when the density increases to 80 veh/km/lane. The saturation of the channel (i.e., the percentage of RBs is very high or close to 100%) increases the latency as observed in Fig. 2.b. These results have highlighted the impact of the MCS to achieve different reliability and spectrum efficiency trade-offs.

Fig. 2 and Fig. 3 show that the latency can significantly increase when the percentage of utilized RBs is high. Fig. 2 corresponds to the latency experienced by the transmitted packets. When the channel is saturated (i.e., the percentage of utilized RBs is close to 100%), certain packets are dropped because they cannot be transmitted before the next packet is generated. The percentage of dropped packets for the LEP and HEP configurations is reported in Table III for densities of 60 and 80 veh/km/lane, all the numerologies, and transmission periods T_p of 50 ms and 20 ms. Table III clearly shows that the HEP configuration results in a significantly higher percentage of packets dropped than the LEP configuration since it significantly increases the utilization of RBs (Fig. 3). Table III shows that the percentage of dropped packets significantly increases as the transmission period T_p decreases. This is the case the utilization of the RBs, and hence the risk of channel saturation, increases as more packets are generated per second and vehicle. This is shown in Fig. 4 that represents the percentage of utilized RBs as a function of the T_p at a traffic density of 60 veh/km/lane. The figure shows that saturation is

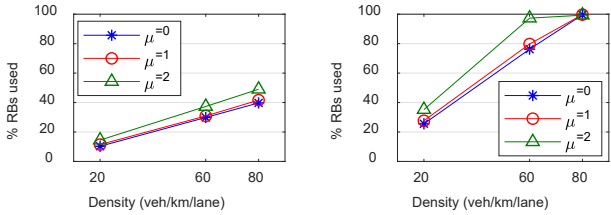
⁴ Symbol time duration decreases as SCS increases, and so does time duration of CP. Due to this fact, higher numerologies are more affected by ISI; this problem appears in scenarios with particularly high delay spread.

This is the case for numerology 2 that considers a 60 kHz SCS, and [3] defines the possibility to use an ECP to better combat ISI only for numerology 2.



a) Low error protection – LEP. b) High error protection – HEP.
Fig. 2. Average latency when transmission period (T_p) is equal to 50 ms.

Numerology (μ)	LEP (BLER target=10%)	HEP (BLER target= 10^{-5})
0	2.46	6.64
1	2.46	6.64
2	2.82	7.66

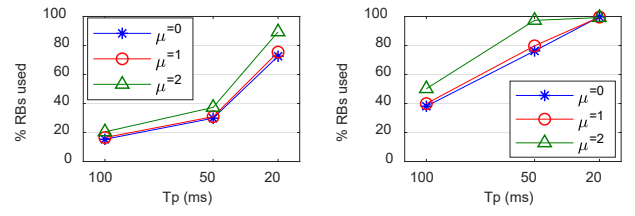


a) Low Error Protection – LEP. b) High Error Protection – HEP.
Fig. 3. Percentage of RBs utilized (transmission period T_p equal to 50 ms).

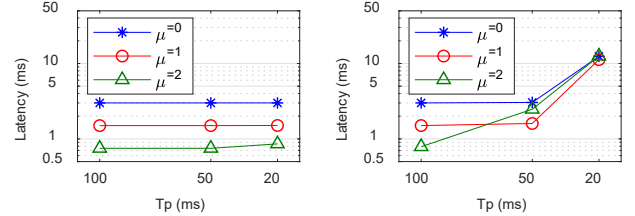
μ	60 veh/km/lane				80 veh/km/lane			
	LEP		HEP		LEP		HEP	
	$T_p=50$	$T_p=20$	$T_p=50$	$T_p=20$	$T_p=50$	$T_p=20$	$T_p=50$	$T_p=20$
0	0.0	0.0	0.0	47.8	0.0	0.0	2.9	61.0
1	0.0	0.0	0.0	49.3	0.0	1.6	5.3	62.1
2	0.0	0.0	0.5	59.3	0.0	17.7	24.2	69.6

reached with HEP and a T_p of 20 ms for all numerologies. This is not the case for T_p equal to 50 ms, which explains why packets are dropped with T_p equal to 20 ms but not with T_p equal to 50 ms when using HEP under a density of 60 veh/km/lane (Table III).

Fig. 2 clearly shows that the numerology has an impact on the latency. Fig. 2.a shows that the latency decreases with higher numerologies for the LEP configuration. This is because higher numerologies reduce the time duration of slots. A similar effect is observed with the HEP configuration when the density is low (20 veh/km/lane). When the density increases, the latency augments with HEP for all the numerologies analyzed. However, the increase is larger for the highest numerologies. This is because when the numerology increases, the SCS augments and the number of RBs per slot is smaller for a fixed bandwidth, and it is then more difficult to find the necessary number of free RBs in a slot to transmit a packet. This, in turn, increases the latency, in particular for the packets that require a higher number of RBs. The high increase in latency observed with HEP and numerology 2 when the density increases is also due to the use of the ECP that reduces the number of OFDM symbols per slot to only 12 compared to 14 in the case of the NCP. This augments the number of RBs needed (on average) to transmit a packet with numerology 2 and ECP compared to numerology 0 or 1 and NCP (see Table II). The impact of numerology 2 with ECP with high vehicular densities is also observed in Table III. The table shows that the percentage of dropped packets with HEP,



a) Low error protection – LEP b) High error protection – HEP
Fig. 4. Percentage of utilized RBs as a function of the transmission period T_p (60 veh/km/lane).



a) Low error protection – LEP b) High error protection – HEP
Fig. 5. Average latency as a function of the transmission period T_p (60 veh/km/lane).

$T_p=50$ ms and 80 veh/km/lane is equal to 2.9% and 5.3% for numerologies 0 and 1 respectively, and increases to 24.2% for numerology 2.

Fig. 4 illustrated the impact of T_p on the percentage of utilized RBs. Fig. 5 quantifies the impact of T_p on the average latency. Fig. 5.a shows that the average latency does not significantly vary with T_p when using LEP (see Fig. 5.a). This is despite an increase of the percentage of utilized RBs (but still below saturation) when T_p decreases to 20 ms as observed in Fig. 4.a. However, T_p has an important impact on latency when using a high error protection (HEP) that is particularly relevant for numerology 2. For example, Fig. 5.b shows that the latency increases a 214% for numerology 2 when T_p decreases from 100 ms to 50 ms, while it remains constant for numerologies 0 and 1. This is because numerology 2 reaches channel saturation faster than the rest of numerologies (Fig. 4.b). Augmenting the channel load by decreasing T_p to 20 ms affects all numerologies with HEP: the latency considerably increases (by a factor higher than 4, Fig. 5.b) and so does the percentage of dropped packets (over 50% of packets are dropped for each numerology, Table III).

The previous results have analyzed the impact of 5G RAN configurations on the performance, and in particular on the latency. We now determine whether these 5G RAN configurations can satisfy the requirements for the cooperative lane change service with low and high levels of automation. The LLoA automation configuration requires that 90% of the transmitted packets are successfully delivered in less than 25 ms, while HLoA automation configuration requires that 99.99% of the transmitted packets are received in less than 10 ms. Table IV and Table V report the maximum UL+DL RAN latency experienced by 90% and 99.99% of the packets, respectively. Table IV shows results for the LEP and HEP configurations, while Table V only shows results for HEP since the LEP configuration has a target BLER of 10% and hence cannot guarantee the reliability requirement of 99.99% due to propagation errors. The mark ‘-’ in the tables means that the corresponding configuration was not able to meet the reliability requirement, i.e., the percentage of packets lost (due to propagation errors) or dropped at the transmitter is higher than the maximum permitted to meet the reliability

TABLE IV
MAXIMUM LATENCY (UL+DL) IN MS EXPERIENCED BY THE 90% OF THE PACKETS

T_p (ms)	LEP (BLER target=10%)									HEP (BLER target=10 ⁻⁵)								
	20 veh/km/lane			60 veh/km/lane			80 veh/km/lane			20 veh/km/lane			60 veh/km/lane			80 veh/km/lane		
	$\mu=0$	$\mu=1$	$\mu=2$	$\mu=0$	$\mu=1$	$\mu=2$	$\mu=0$	$\mu=1$	$\mu=2$	$\mu=0$	$\mu=1$	$\mu=2$	$\mu=0$	$\mu=1$	$\mu=2$	$\mu=0$	$\mu=1$	$\mu=2$
100	4	2	1	4	2	1	4	2	1	3.8	2	1	3.8	2	1	3.8	2	1.2
50	4	2	1	4	2	1	4	2	1.2	3.8	2	1	3.8	2	4.8	8.2	9.6	-
20	4	2	1	4	2.2	7.6	-	-	-	3.8	2	1.6	-	-	-	-	-	-

TABLE V
MAXIMUM LATENCY (UL+DL) IN MS EXPERIENCED BY THE 99.99% OF THE PACKETS WITH HEP CONFIGURATION (BLER TARGET=10⁻⁵)

T_p (ms)	20 veh/km/lane			60 veh/km/lane			80 veh/km/lane		
	$\mu=0$	$\mu=1$	$\mu=2$	$\mu=0$	$\mu=1$	$\mu=2$	$\mu=0$	$\mu=1$	$\mu=2$
100	4	2	1.6	4	2.4	2.2	4.2	2.6	4.2
50	4	2	1.8	6.2	7.2	-	-	-	-
20	4.6	4.4	18	-	-	-	-	-	-

requirement (e.g., higher than 10% for the low level of automation configuration of the cooperative lane change service). Table IV shows that the service requirements for LLoA can be satisfied with many of the RAN configurations analyzed (numerology, error protection and T_p) under different densities. The service requirements cannot be met only under the highest loads, i.e. for the lowest T_p (20 ms) and the highest vehicle density analyzed. The service requirement cannot be met also with a density of 60veh/km/lane and $T_p=20$ ms when using HEP. Table IV shows that it is possible to achieve maximum latency values significantly lower than the 25 ms latency limit. However, we should note that the end-to-end latency does not only depend on the RAN latency but also on the latency at the transport and core networks. In any case, reducing the latency at the RAN provides a better way to ultimately comply with the end-to-end latency requirement. Table V shows that the HEP configuration can only satisfy the HLoA service requirements with low/medium traffic loads, i.e. for combinations of low/medium vehicular density values and medium/high T_p . The numerology 2 is also not capable to meet the requirements for certain low load scenarios. The percentage of packets lost due to propagation errors or dropped at the transmitter is lower than 0.01% in scenarios with 20 veh/km/lane, $T_p=20$ ms and numerology 2. However, the latency experienced for some packets is higher than 10 ms as shown in Table V. We should also note that in many scenarios the RAN latency is above 4 ms which leaves less than 6 ms to the core and transport networks to ultimately comply with the HLoA end-to-end latency requirement.

V. CONCLUSIONS

This study has evaluated the impact of the 5G NR configuration on the scalability of 5G networks that support advanced V2X services with different requirements based on the level of automation of CAVs (Connected and Automated Vehicles). In particular, the study has analyzed the performance that can be achieved with different 5G NR numerologies, slot durations, cyclic prefixes, and modulation and coding schemes, as the network scales with the density of vehicles and the traffic load generated per vehicle. The study has shown that higher numerologies achieve lower latencies under low to moderate network loads. However, higher numerologies require larger bandwidth, and this results in a faster increase in the latency when the network load increases. This paper has also shown that the use of the extended CP results in less efficient use of radio resources that decreases the traffic load that can be supported in the system. The study has also highlighted the impact of the MCS and the resulting spectrum efficiency and reliability trade-offs. The conducted

analysis shows that the most robust MCSs can support V2X services with higher levels of automation and more stringent requirements. This is done at the expense of the density of vehicles that can be supported as the latency increases rapidly with the traffic load. Higher traffic loads are supported with less robust MCSs, but such MCSs can only support V2X services with lower requirements and lower levels of automation as defined in 3GPP. The conducted analysis shows that the capacity of 5G to support eV2X services with diverse requirements strongly depends on the traffic load and the NR configuration that must be carefully selected.

ACKNOWLEDGMENT

UMH work was supported in part by the Spanish Ministry of Science and Innovation (MCI), AEI and FEDER funds under Project TEC2017-88612-R, and the Ministry of Universities (IJC2018-036862-I), and the Generalitat Valenciana.

REFERENCES

- [1] 3GPP TR 37.910 V16.1.0, "Technical Specification Group Radio Access Network; Study on self evaluation towards IMT-2020 submission (Release 16)", September 2019.
- [2] K. Serizawa, et al., "Field Trial Activities on 5G NR V2V Direct Communication Towards Application to Truck Platooning", in *Proc. of the 2019 IEEE 90th Vehicular Technology Conference (VTC2019-Fall)*, Honolulu, HI, USA, 2019, pp. 1-5.
- [3] N. Patriciello, et al., "5G New Radio Numerologies and their Impact on the End-To-End Latency", in *Proc. of the 2018 IEEE 23rd International Workshop on Computer Aided Modeling and Design of Communication Links and Networks*, Barcelona, 2018, pp. 1-6.
- [4] M.C. Lucas-Estañ, et al., "On the Scalability of the 5G RAN to Support Advanced V2X Services", in *Proc. of the 2020 IEEE Vehicular Networking Conference (VNC)*, Virtual Conference, Dec. 2020.
- [5] 3GPP TS 38.211 V16.1.0, "Technical Specification Group Radio Access Network; NR; Physical channels and modulation (Release 16)", March 2020.
- [6] 3GPP TS 38.214 V16.1.0, "Technical Specification Group Radio Access Network; NR; Physical layer procedures for data (Release 16)", March 2020.
- [7] 3GPP TS 38.104 V16.2.0, "Technical Specification Group Radio Access Network; NR; Base Station (BS) radio transmission and reception (Release 16)", March 2020.
- [8] ITU Radiocommunication Study Groups, "Final Evaluation Report from the 5G Infrastructure Association on IMT-2020 Proposals IMT-2020/14, 15, 16 parts of 17", Document 5D/50-E, Feb. 2020.
- [9] 3GPP TS 22.186 V16.2.0, "Technical Specification Group Services and System Aspects; Enhancement of 3GPP support for V2X scenarios; Stage 1 (Release 16)", June 2019.
- [10] B. Lehmann, H. Günther and L. Wolf, "A Generic Approach towards Maneuver Coordination for Automated Vehicles", in *Proc. of the 2018 21st International Conference on Intelligent Transportation Systems (ITSC)*, Maui, HI, 2018, pp. 3333-3339.
- [11] M. Sepulcre, et al., "On the Potential of V2X Message Compression for Vehicular Networks", *IEEE Access*, vol. 8, pp. 214254-214268, Nov. 2020.
- [12] 3GPP TR 38.913 V15.0.0, "Technical Specification Group Radio Access Network; Study on Scenarios and Requirements for Next Generation Access Technologies; (Release 15)", June 2018.
- [13] 3GPP, RP-201038, "WID revision: NR Multicast and Broadcast Services", 3GPP TSG-RAN Meeting #88-e, July 2020.